THE ASTROPHYSICAL JOURNAL, 523:328–339, 1999 September 20

CORRELATED ERRORS IN *HIPPARCOS* PARALLAXES TOWARD THE PLEIADES AND THE HYADES

VIJAY K. NARAYANAN AND ANDREW GOULD[1]
Department of Astronomy, Ohio State University, Columbus, OH 43210; vijay@astronomy.ohio-state.edu, gould@astronomy.ohio-state.edu
Received 1998 October 21; accepted 1999 May 6

ABSTRACT

We show that the errors in the *Hipparcos* parallaxes toward the Pleiades and the Hyades open clusters are spatially correlated over angular scales of 2°–3°, with an amplitude of up to 2 mas. This correlation is stronger than expected based on the analysis of the *Hipparcos* catalog. We predict the parallaxes of individual cluster members, $\pi_{\rm pm}$, from their *Hipparcos* proper motions, assuming that all the cluster members move with the same space velocity. We compare these parallaxes with their *Hipparcos* parallaxes, $\pi_{\rm Hip}$, and find that there are significant spatial correlations in the latter quantity. We derive a distance modulus to the Pleiades of 5.58 ± 0.18 mag from the gradient in the radial velocities of the Pleiades members in the direction parallel to the proper motion of the cluster. This value, derived using a geometric method, agrees very well with the distance modulus of 5.60 ± 0.04 mag determined using the main-sequence fitting technique, compared with the value of 5.33 ± 0.06 mag inferred from the average of the *Hipparcos* parallaxes of the Pleiades members. We show that the difference between the main-sequence fitting distance and the *Hipparcos* parallax distance can arise from spatially correlated errors in the *Hipparcos* parallaxes of individual Pleiades members. Although the *Hipparcos* parallax errors toward the Hyades are spatially correlated in a manner similar to those of the Pleiades, the center of the Hyades is located on a node of this spatial structure. Therefore, the parallax errors cancel out when the average distance is estimated, leading to a mean Hyades distance modulus that agrees with the pre-*Hipparcos* value. We speculate that these spatial correlations are also responsible for the discrepant distances that are inferred using the mean *Hipparcos* parallaxes to some open clusters, although an agreement between the mean *Hipparcos* parallax distance and the main-sequence fitting distance to other clusters does not necessarily preclude spatially correlated *Hipparcos* parallax errors. Finally, we note that our conclusions are based on a purely geometric method and do not rely on any models of stellar isochrones.

Subject headings: astrometry — open clusters and associations: individual (Pleiades, Hyades) — stars: distances

1. INTRODUCTION

Trigonometric parallax is a fundamental method for measuring distances to astronomical objects and is the first rung of the cosmic distance ladder. It is a purely geometric technique, without the need for any ill-understood empirical correlations between two physical quantities, one of which is dependent on the distance and the other independent of distance. The *Hipparcos* Space Astrometry Mission (ESA 1997) has derived accurate absolute trigonometric parallaxes for about 120,000 stars distributed all over the sky and has produced the largest homogeneous all-sky astrometric catalog to date. The global systematic errors in the *Hipparcos* parallaxes are estimated to be $\lesssim 0.1$ mas, while the random errors in parallaxes of individual stars are typically on the order of 1 mas (Arenou et al. 1995; Arenou, Mignard, & Palasi 1997; Lindegren 1995). However, the mean *Hipparcos* parallax distances to some open clusters are different from their distances inferred using other techniques (Mermilliod et al. 1997b; Robichon et al. 1997; van Leeuwen & Ruiz 1997), suggesting that the true systematic errors may be an order of magnitude larger, at least on small angular scales (Pinsonneault et al. 1998, hereafter PSSKH98). In this paper, we estimate the level of the systematic errors in the *Hipparcos* parallaxes toward the Pleiades and the Hyades clusters by comparing for each of the cluster members, its *Hipparcos* parallax distance with its relative distance inferred from its *Hipparcos* proper motion, assuming that all the cluster members move with the same bulk velocity. We first determine the distance to the Pleiades cluster using a variant of the moving cluster method and then present the evidence for spatial correlations in the *Hipparcos* parallaxes toward both the Pleiades and the Hyades.

The distances to the Hyades and the Pleiades are fundamental quantities in establishing the absolute level of the main-sequence in the H-R diagram and, hence, in estimating the distances to open clusters using the main-sequence fitting technique. Thereby, they provide the first calibration points in the extragalactic distance scale. Hence, it is imperative that these distances are firmly established using techniques that require minimal assumptions. While the *Hipparcos* astrometric catalog provides straightforward distance estimates to these clusters from the mean of the parallaxes of the cluster members, there are surprising differences between the mean *Hipparcos* parallax distances and the distances estimated using other techniques for some open clusters, including the Pleiades (Mermilliod et al. 1997b; Robichon et al. 1997). In particular, the distance modulus to the Pleiades derived using the mean of the *Hipparcos* parallaxes is almost 0.3 mag smaller than that derived using the main-sequence fitting technique (van Leeuwen & Ruiz 1997), while there is no such discrepancy for the Hyades (Perryman et al. 1998; PSSKH98). A confirmation of this 15% shorter distance to the Pleiades from the *Hipparcos* parallaxes has serious implications for our understanding of stellar evolution. For example, if the Pleiades stars are in fact 0.3 mag fainter than they were previously thought to be,

[1] Alfred P. Sloan Foundation Fellow.

there must be a population of subluminous zero-age main-sequence field stars in the solar neighborhood that has so far escaped detection (Soderblom et al. 1998).

The difference in the distance estimates using the *Hipparcos* parallaxes and using the main-sequence fitting method are much larger than what would be expected from incorrect metallicities, and this has led to an active search for alternate explanations. These alternatives range from the "Hyades anomaly" (Crawford 1975) arising from a low helium abundance of the Hyades (Stromgren, Olsen, & Gustafsson 1982), which therefore affects the relative distance between the Hyades and the Pleiades, to the "fourth parameter" effect, which states that a fourth parameter is required, in addition to the age, the metallicity, and the helium abundance, to adequately describe solar-type stars (Alexander 1986; Nissen 1988; see Mermilliod et al. 1997b for a review of explanations invoking all these different effects). PSSKH98 showed that an impossibly large helium abundance ($Y = 0.37$) is required for the Pleiades stars to reconcile the shorter value of the Pleiades distance inferred from the *Hipparcos* parallaxes with the main-sequence fitting distance and proposed a simpler explanation that there are spatial correlations in the *Hipparcos* parallax errors on small angular scales. All these drastic consequences of a shorter distance to the Pleiades mean that we need to check independently if the *Hipparcos* parallaxes toward this cluster are free from any systematic errors, before invoking alternate explanations for the "failure" of the main-sequence fitting technique.

Here, we compare the *Hipparcos* parallax distances to the members of the Pleiades and the Hyades clusters with their distances computed using the moving cluster method. This method assumes that all the cluster members move with the same space velocity and that the velocity structure of the cluster is not significantly affected by rotation. Under this assumption, we can predict the distance (and hence the parallax) to each of the individual cluster members if we know the common space velocity of the cluster. We use a variant of the moving cluster method, the radial velocity gradient method, to compute the distance to the Pleiades using simple geometrical considerations. We use this distance to estimate the common space velocity of all the Pleiades members and then predict the parallaxes of individual Pleiades members. We then compare these parallaxes with the *Hipparcos* parallaxes of the same stars. This enables us to test the accuracy of the *Hipparcos* parallaxes on small scales, in a manner that is independent of any stellar isochrones. We extend this analysis to the Hyades cluster using the common cluster space velocity determined by Narayanan & Gould (1999, hereafter NG99). The principal result of this paper is that the *Hipparcos* parallaxes toward both the clusters are correlated with position on scales of about 3°, with an amplitude of about 1–2 mas. While it is well known that the errors in the *Hipparcos* parallaxes are correlated over small angular scales (Lindegren 1988, 1989; Lindegren, Froeschle, & Mignard 1997; Arenou 1997; van Leeuwen & Evans 1998), we find that the correlation is probably stronger than previous estimates.

The outline of this paper is as follows. We explain the different variants of the moving cluster method in § 2. We describe our selection of Pleiades cluster members from the *Hipparcos* catalog and our estimate of the average proper motion of the cluster in § 3. In § 4, we derive the distance to the Pleiades from the gradient in the radial velocities of its members, in the direction parallel to the proper motion of the cluster. We compare this distance with the mean *Hipparcos* parallax distance and give our estimates of the systematic errors in *Hipparcos* parallaxes toward the Pleiades in § 5. In § 6, we show that the same type of systematic errors are also present in the *Hipparcos* parallaxes toward the Hyades. We present our conclusions in § 7. This is the second paper in the series in which we compare the *Hipparcos* parallaxes of open clusters with independent distances derived using geometrical techniques, the first being a check of the *Hipparcos* systematics toward the Hyades (NG99). We note that we will drop the usual conversion factor $A_v = 4.74047$ km yr s^{-1} from all our equations for the sake of clarity, leaving it to the reader to include it in the appropriate equations. This is equivalent to adopting the units of AU yr^{-1} for the velocities, although we will still quote the numerical values of the velocities in km s^{-1}.

2. MOVING CLUSTER METHODS

The fundamental requirement for using the moving cluster method to estimate the distance to a stellar cluster is that all the stars in the cluster have the same space velocity ($\boldsymbol{V}$) to within the velocity dispersion of the cluster. The three observables of the cluster members, namely, their radial velocities (V_r), their proper motion vectors ($\boldsymbol{\mu}$), and their angular separations ($\boldsymbol{\theta}$) from a suitably defined cluster center, are to a good approximation related by

$$\boldsymbol{V}_T = \boldsymbol{V} - V_r \hat{\boldsymbol{r}} , \tag{1}$$

$$\boldsymbol{\mu} = \frac{\boldsymbol{V}_T}{d} , \tag{2}$$

$$\delta \boldsymbol{V}_T = -V_r \boldsymbol{\theta} , \tag{3}$$

$$\delta \mu_\perp = -\left(\frac{V_r}{d}\right)\theta_\perp , \tag{4}$$

$$\delta \mu_\parallel = -\left(\frac{V_r}{d}\right)\theta_\parallel - \left(\frac{\delta d}{d}\right)\mu_\parallel , \tag{5}$$

and

$$\delta V_r = (\boldsymbol{\theta} \cdot \boldsymbol{\mu}) d = \theta_\parallel \mu_\parallel d = \theta_\parallel V_T , \tag{6}$$

where $\boldsymbol{V}_T$ is the transverse velocity of the cluster member in the plane of the sky, $V_T = |\boldsymbol{V}_T|$, the subscript $\perp(\parallel)$ for the quantities μ and θ refers to the components of the respective vectors perpendicular (parallel) to the proper motion vector, and δx is the difference in quantity x ($x = \boldsymbol{V}_T, \mu_\perp, \mu_\parallel, d$) between the individual member star and its average value at the centroid of the cluster sample. Equations (1)–(6) assume that $|\boldsymbol{\theta}| \ll 1$ (the small angle approximation), that $(\delta d/d) \ll 1$, that the velocity dispersion of the cluster is small compared to its mean space velocity, and that the velocity structure of the cluster is not significantly affected by rotation, expansion, shear, etc. Equations (4), (5), and (6) give three independent measures of the distance to the cluster center, and we can derive a more accurate distance to the cluster by taking their weighted average. This can be effectively accomplished using the statistical parallax formalism, as explained by NG99.

The two variants of the moving cluster method that are currently in use depending on the nature of the available data are the following.

1. *The convergent-point method.*—The proper motions of the individual cluster members are used to derive a convergent point on the sky. This information is combined with the average radial velocity of the cluster center to derive its distance using equation (4). This method has been successfully applied to the Hyades cluster for a very long time (Boss 1908; Schwan 1991; Perryman et al. 1998). Moreover, if there is independent information from high-precision photometry about the relative distances between individual cluster members, equation (5) can also be used to derive a more precise estimate of the cluster distance (NG99).

2. *The radial velocity gradient method.*—The radial velocities of the individual cluster members can be used to measure the gradient in the radial velocity across the face of the cluster, in the direction parallel to the proper motion of the cluster. This can be combined with an estimate of the average cluster proper motion, to derive the cluster distance using equation (6). This technique was first used by Thackeray (1967) to derive the convergent point of the Scorpio-Centaurus association. It has since been applied to determine the distance to the Hyades cluster (Detweiler et al. 1984; Gunn et al. 1988) and to determine the convergent point of the Pleiades cluster by assuming a distance (Rosvick, Mermilliod, & Mayor 1992a).

The three equations (4), (5), and (6) yield independent measures of the distance to the cluster with relative weights $W_i = N_i(d_i/\sigma_i)^2$, where d_i and σ_i, $(i = 1, 2, 3)$ are the three distances and distance errors and N_i is the number of stars used to estimate the cluster distance by method i. These weights are approximately given by

$$W_1 = N\left\langle \frac{(\theta_\perp V_r)^2}{(d\sigma_\mu)^2 + \sigma_{\rm clus}^2} \right\rangle , \tag{7}$$

$$W_2 = N\left\langle \frac{(\theta_\parallel V_r)^2}{(d\sigma_\mu)^2 + \sigma_{\rm clus}^2 + (\sigma_d\,\mu)^2} \right\rangle , \tag{8}$$

and

$$W_3 = N\left\langle \frac{(\theta_\parallel V_T)^2}{\sigma_r^2 + \sigma_{\rm clus}^2} \right\rangle , \tag{9}$$

where σ_r and σ_μ are the errors in the radial velocities and the proper motion, respectively, σ_d is the uncertainty in the relative distance to individual cluster members, and $\sigma_{\rm clus}$ is the velocity dispersion of the cluster. The weight W_1 corresponds to the classical convergent-point moving cluster method using individual proper motions (eq. [4]), while W_2 corresponds to the extension of this method using photometry to estimate the relative distances between the cluster members (eq. [5]). The weight W_3 corresponds to the radial velocity gradient method described by equation (6).

For the purpose of illustration, we assume that for the Pleiades cluster, $\sigma_{\rm clus} = 0.7$ km s^{-1}, $d\sigma_\mu = 0.9$ km s^{-1}, $\sigma_r = 0.3$ km s^{-1}, $\sigma_d\,\mu = 0.9$ km s^{-1}, $\langle\theta_\parallel^2\rangle = \langle\theta_\perp^2\rangle \equiv \langle\theta^2\rangle$, $V_r = (1/5)V_T = 6$ km s^{-1}, and $N_3 = 2N_2 = 2N_1 = 140$. This leads to $W_1 : W_2 : W_3 = 0.009 : 0.005 : 1.0$, which shows that 99% of the information about the Pleiades cluster distance is in equation (6), i.e., in the radial velocity gradient method. We will therefore use only the radial velocity gradient method in this paper. This is in sharp contrast to the situation for the Hyades where the relative weights are in the ratio 1 :0.33 :0.50, and hence most of the distance information is in the classical convergent point method as extended by NG99.

3. MEMBERSHIP AND AVERAGE PROPER MOTION

The procedure for determining the distance to the Pleiades from the radial velocity gradient (eq. [6]) requires an accurate estimate of the average proper motion of the cluster center in an inertial frame. In this section, we explain our procedure for selecting Pleiades members from the *Hipparcos* catalog and our estimate of the location and the average proper motion of the centroid of these members.

3.1. *Cluster Membership*

We begin by selecting all the stars from the *Hipparcos* catalog that are within 10° of an approximate center of the Pleiades cluster and whose proper motions are consistent with them being Pleiades members. We assume an average radial velocity at the cluster center of 5 km s^{-1}, an average proper motion of $\mu_\alpha = 20$ mas yr^{-1}, $\mu_\delta = -45$ mas yr^{-1}, an average distance of $d = 132$ pc and an isotropic cluster velocity dispersion of $\sigma_{\rm clus} = 0.8$ km s^{-1}. These values are only representative of the true values and are as such only approximately correct, although we find that the final list of cluster members is not very sensitive to these values. For each star i, we predict its proper motion $\boldsymbol{\mu}_{{\rm pred},i}$ using equations (1) and (2) and compute the quantity χ_i^2, defined as

$$\chi_i^2 = \langle \Delta\boldsymbol{\mu}_i \,|\, \boldsymbol{C}_i^{-1} \,|\, \Delta\boldsymbol{\mu}_i \rangle , \tag{10}$$

where $\Delta\boldsymbol{\mu}_i = (\boldsymbol{\mu}_{{\rm Hip},i} - \boldsymbol{\mu}_{{\rm pred},i})$, $\boldsymbol{\mu}_{{\rm Hip},i}$ is its *Hipparcos* proper motion, and where we have employed Dirac notation,

$$\langle X \,|\, \mathcal{O} \,|\, Z \rangle = \sum_{i,j} X_i \mathcal{O}_{ij} Z_j . \tag{11}$$

The covariance matrix $\boldsymbol{C}_i$ is the sum of three terms: (1) the covariance matrix of the *Hipparcos* proper motion; (2) the isotropic velocity dispersion tensor of the cluster divided by the square of the mean distance of the cluster, $(\sigma_{\rm clus}/d)^2$; and (3) a matrix of the form $\theta_d^2(\boldsymbol{\mu}^T\boldsymbol{\mu})_{{\rm pred},i}$, where we adopt $\theta_d \equiv (\delta d/d) = 6\%$. The third term accounts for a finite depth of the Pleiades cluster along the radial direction and allows a Pleiades member to be located either in front of or behind the assumed fiducial distance d. We select all the stars with $\chi_i^2 \le 9$ (corresponding to 3 σ) to be candidate Pleiades members. This procedure selects a total of 81 Pleiades candidates from the *Hipparcos* catalog. These include all but 12 of the 74 Pleiades candidate stars in the *Hipparcos* Input Catalog. The proper motions of these 12 stars (with *Hipparcos* identifications HIP 16119, 17026, 17684, 17759, 17832, 18018, 18046, 18106, 18149, 18201, 18748, and 19496) differ widely from the average proper motion of the Pleiades, and they are therefore most likely to be nonmembers.

We predict the parallax of each of these Pleiades candidates using its *Hipparcos* proper motion and the average space velocity of the cluster as

$$\pi_{{\rm pm},i} = \frac{\langle (\boldsymbol{V}_t)_i \,|\, \boldsymbol{C}_i^{-1} \,|\, \boldsymbol{\mu}_{{\rm Hip},i} \rangle}{\langle (\boldsymbol{V}_t)_i \,|\, \boldsymbol{C}_i^{-1} \,|\, (\boldsymbol{V}_t)_i \rangle} , \tag{12}$$

where $(\boldsymbol{V}_t)_i = \boldsymbol{V}_c - (\hat{\boldsymbol{r}}_i \cdot \boldsymbol{V}_c)\hat{\boldsymbol{r}}_i$ is the transverse velocity of the cluster in the plane of the sky at the position of the star i, and the covariance matrix $\boldsymbol{C}_i$ is the sum of the velocity dispersion tensor of the cluster divided by the square of the mean distance to the cluster and the covariance matrix of the *Hipparcos* proper motion of star i. The error in $\pi_{{\rm pm},i}$ is

equal to $\langle (\boldsymbol{V}_t)_i | \boldsymbol{C}_i^{-1} | (\boldsymbol{V}_t)_i \rangle^{1/2}$. We use this parallax and the V_J magnitude from Tycho photometry to estimate the absolute magnitude (and the associated error) of each of these Pleiades candidates.

Figure 1 shows the color-magnitude diagram (CMD) of all these Pleiades candidates. There is an easily identifiable main sequence in the color range $0 < (B-V)_J < 0.9$, and there are a few stars that clearly lie either above or below this sequence even after accounting for their magnitude errors. We adopt a color-magnitude relation

$$M_V = 4 + 5.57[(B-V)_J - 0.5] \quad (13)$$

in the color range $0 < (B-V)_J < 0.9$ and accept all the stars that lie within 0.4 mag of this line as Pleiades members. The observed color-magnitude relation is quite steep for $(B-V)_J < 0$ and does not show an unambiguous main sequence. Therefore, we assume that all the stars with $(B-V)_J \leq 0$ are Pleiades members. We also reject one star (HIP 16431) whose error in proper motion is greater than 4 mas yr^{-1}. This algorithm selects a total of 65 stars as Pleiades members from the *Hipparcos* catalog. These members are shown as filled circles in Figure 1, while the nonmembers and plausible binary systems are represented by the open circles. To summarize our selection of Pleiades members, we first select a total of 81 candidates from the *Hipparcos* catalog whose proper motions are consistent with them being Pleiades members. We predict their parallaxes from their *Hipparcos* proper motions assuming that they have the same space velocity as the centroid of the Pleiades. We then enforce a photometric cut where we accept as Pleiades members only those 65 candidates that lie close to the Pleiades main-sequence in the color-magnitude diagram.

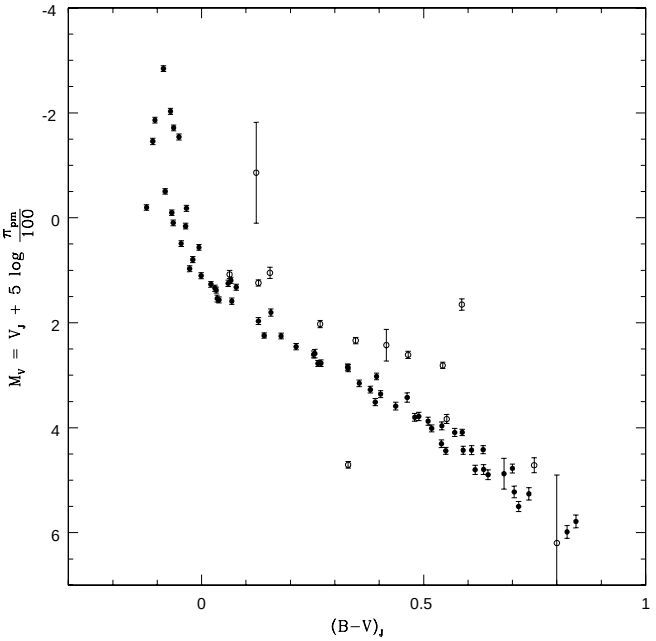

FIG. 1.—Color-magnitude diagram of all the stars in the *Hipparcos* catalog whose individual proper motions are consistent with them being Pleiades members. The parallax to each star is estimated from its *Hipparcos* proper motion, assuming a common space velocity for all the Pleiades members. The filled circles show the stars used to derive the average proper motion of the Pleiades, while the open circles represent nonmembers and plausible binaries. The colors and apparent magnitudes $(B-V)_J$ and V_J are taken from Tycho photometry.

3.2. *Average Proper Motion*

We estimate the centroid and the average proper motion of the Pleiades cluster using all the 65 Pleiades members identified from the *Hipparcos* catalog in § 3.1. We compute the average proper motion at the cluster center as the mean of all the individual proper motions of the Pleiades members weighted inversely by their covariance matrices. The covariance matrix of each star is the sum of the covariance matrix of the *Hipparcos* proper motions, the diagonal velocity dispersion tensor divided by the square of the mean distance of the cluster $(\sigma_{\rm clus}/d)^2$ and a term arising from the distance "dispersion" $(\sigma_d/d)^2)\boldsymbol{\mu}^T \cdot \boldsymbol{\mu}$ to account for the nonzero depth of the Pleiades cluster. The observed dispersion in the proper motions of the cluster members in the direction perpendicular to the proper-motion vector includes contributions from only the velocity dispersion term and the errors in the *Hipparcos* proper motions, while the observed dispersion parallel to the proper motion vector includes, in addition, a contribution from the dispersion in the distances to individual Pleiades members. Therefore, we estimate the dispersion in the proper motions from the difference between the observed and the *Hipparcos* proper-motion covariance matrices in the perpendicular direction and derive the distance dispersion as the difference between the observed covariance matrices in the parallel and the perpendicular directions.

We find that the equatorial coordinate of the centroid of all the 65 Pleiades members is $\alpha = 03^{\rm h}46^{\rm m}20^{\rm s}$, $\delta = 23°37'.0$ (2000). The average proper motion of the cluster at this location is $\overline{\mu}_\alpha = 19.79 \pm 0.27$ mas yr^{-1}, $\overline{\mu}_\delta = -45.39 \pm 0.29$ mas yr^{-1}, and the correlation coefficient is -0.087. Our estimate of the average proper motion of the Pleiades agrees well with the estimate of $\overline{\mu}_\alpha = 19.67 \pm 0.24$ mas yr^{-1}, $\overline{\mu}_\delta = -45.55 \pm 0.19$ mas yr^{-1} by van Leeuwen & Ruiz (1997). We repeat the entire cluster-membership determination from the *Hipparcos* catalog stars using this improved estimate of the average cluster proper motion and find that the membership does not change, showing that our selection of Pleiades members is not very sensitive to the initial values we have assumed for the average cluster proper motion. Therefore, we will use these values for the average proper motion of the Pleiades cluster in the remainder of this paper.

In our solution for the average proper motion of the Pleiades, the dispersion in the proper motions is $(\sigma_d/d) = 1.63 \pm 0.38$ mas yr^{-1}. Assuming a distance to the Pleiades of $d = 130.7$ pc (as we will find below), this dispersion in the proper motion corresponds to a velocity dispersion of 1.00 ± 0.24 km s^{-1}, in reasonable agreement with the value of 0.69 ± 0.05 km s^{-1} we infer in § 4.2 from the radial velocities of the Pleiades members. Similarly, we find a value of the distance dispersion of $(\mu\sigma_d/d) = 1.37 \pm 0.74$ mas yr^{-1} from the proper motions, corresponding to a depth of the cluster of $(\sigma_d/d) = (2.77 \pm 1.49)\%$, which in angular scales is $\langle \theta_d^2 \rangle^{1/2} = 1°.59 \pm 0°.85$. This is also in agreement with the angular dispersion of the 65 cluster members in the directions perpendicular and parallel to the average proper motion of the cluster, namely, $\langle \theta_\perp^2 \rangle^{1/2} = 1°.74 \pm 0°.15$ and $\langle \theta_\parallel^2 \rangle^{1/2} = 2°.03 \pm 0°.18$. Thus, the estimates of the cluster velocity dispersion from both the proper motions and the radial velocities (which we will estimate in § 4.2) are consistent with each other. Similarly, the radial extent of the cluster that we infer from the proper motions is also comparable to the angular extent of the 65

members of the Pleiades cluster. We also find that 64 of the 65 Pleiades members are located within 6.°2 of the centroid of the cluster.

4. RADIAL VELOCITY GRADIENT AND CLUSTER DISTANCE

We compute the distance to the Pleiades from the radial velocity gradient method using the average proper motion derived in the previous section and the individual radial velocities of Pleiades members. We now describe our selection of the Pleiades members with radial velocities and our estimate of the distance to the cluster from its gradient in the direction parallel to the average proper motion of the cluster.

4.1. *Radial Velocity Sample*

The Pleiades candidates in the *Hipparcos* catalog are mostly bright, early-type stars with large rotational velocities. Hence, it is difficult to measure their radial velocities from their spectra, and the radial velocity surveys of Pleiades stars have been almost entirely limited to faint, late-type stars (later than the spectral type F). Therefore, we select another list of fainter Pleiades members from the literature with measured radial velocities.

Our principal source of radial velocities is the radial velocity survey of the core and the corona stars in the Pleiades using the CORAVEL radial velocity scanner (Rosvick, Mermilliod, & Mayor 1992a, 1992b; Mermilliod, Bratschi, & Mayor 1997a; Raboud & Mermilliod 1998). These three data sets contain the radial velocity data for, respectively, stars in the Pleiades corona selected on the basis of their proper motions and Walraven photometry by van Leeuwen, Alphenaar, & Brand (1986), stars in the outer regions of the cluster selected on the basis of their proper motions by Artyukhina & Kalinina (1970), and stars in the inner region of the Pleiades in the Hertzsprung catalog (Hertzsprung 1947). The radial velocities quoted in the three sources are the raw values measured from the spectra of these stars (J. C. Mermilliod 1998, private communication). In practice, however, the measured radial velocities might include contributions from nonastrometric sources such as convective and gravitational line shifts, atmospheric pulsations etc. (Dravins, Larsson, & Nordlund 1986; Nadeau 1988). The measured radial velocities must be corrected for all these effects to estimate the true astrometric radial velocities of the stars. However, these corrections are likely to be smaller than 1 km s^{-1}; therefore, we do not correct for these effects. Further, it is possible that the three different sources of radial velocities have different zero points, although this is unlikely to be a major problem for our sample of radial velocity stars as all the radial velocities are measured using the same instrument. We note here that our estimate of the distance to the Pleiades using the radial velocity gradient method is insensitive to the absolute zero point of the radial velocities, as long as it is the same for the three data sets.

We reject all the stars from these three data sets that are either known or suspected to be binary systems and that do not have any orbital solutions. We include all the single stars and all the binary systems whose orbits are either known from radial velocity studies (Mermilliod et al. 1992) or can be adequately constrained from infrared imaging (Bouvier, Rigaut, & Nadeau 1997). For the nine infrared binaries, we add an extra error in quadrature of $\epsilon_b = [M_2/(M_1 + M_2)][G(M_1 + M_2)/3a]^{1/2}$ to the quoted errors to reflect the uncertainty arising from the perturbative influence of the nonzero mass of the secondary stars (masses adopted from Bouvier et al. 1997), and we accept only the five stars with $\epsilon_b \leq 0.4$ km s^{-1} as Pleiades candidates. Here, M_1 and M_2 are the masses of the primary and the secondary stars, a is the projected separation of the binary, and the factor of $\sqrt{3}$ in the denominator is a fiducial factor that roughly averages over all possible geometries of the binary orbits. This procedure selects a total of 154 Pleiades candidate stars with measured radial velocities.

4.2. *Distance to the Pleiades*

Consider a cluster at a distance d, whose members all move with the same three space velocity, and let $\boldsymbol{n}$ be the direction vector toward the cluster center as defined by the sample used to compute the average proper motion. The observed radial velocity $V_{r,i}$ of any individual member star i located in the direction $\boldsymbol{n}_i$ is related to the average radial velocity of the cluster center $\overline{V}_r$ by

$$V_{r,i} = d(\boldsymbol{\mu} \cdot \boldsymbol{n}_i) + \overline{V}_r(\boldsymbol{n} \cdot \boldsymbol{n}_i) , \tag{14}$$

where $\boldsymbol{\mu}$ is the average proper motion of the cluster. This equation reduces to equation (6) under the small angle approximation, $|\boldsymbol{\theta}| \equiv |\cos^{-1}(\boldsymbol{n}_i \cdot \boldsymbol{n})| \ll 1$, with $\delta V_r \equiv (V_{r,i} - \overline{V}_r)$. Since we determined $\boldsymbol{\mu}$ in § 3.2 for a sample of stars whose centroid is at $\alpha = 03^h46^m20^s$, $\delta = 23°37'.0$ (2000), we must use the same direction for $\boldsymbol{n}$ in the present analysis, even though this is not the centroid of the radial velocity sample.

We use equation (14) to estimate the distance to the Pleiades (d) from the radial velocities of all the Pleiades candidates selected in § 4.1 and the average cluster proper motion derived in § 3.2. For each Pleiades candidate star i, we predict its radial velocity $V_{r,i,\mathrm{pred}}$ at this cluster distance and compute a quantity χ_v^2, defined as

$$\chi_v^2 = \sum_{i=1}^{N} \frac{(V_{r,i} - V_{r,i,\mathrm{pred}})^2}{\sigma_{v,i}^2} , \tag{15}$$

where $\sigma_{v,i}$ is the sum in quadrature of the errors in the observed radial velocity of star i and the velocity dispersion of the cluster (σ_{clus}) and N is the number of Pleiades candidates. We adjust the value of σ_{clus} so that the total value of χ_v^2 is equal to $(N - 2)$, and reject as nonmembers all the stars whose individual contributions to χ_v^2 is greater than 9 (corresponding to a 3 σ outlier). We repeat this procedure with the reduced list of candidates until there are no stars whose individual contributions to χ_v^2 are greater than 9.

We adopt as Pleiades members all the 141 of the 154 candidate stars that remain after the last iteration and derive a distance to the Pleiades of $d = 130.7 \pm 11.1$ pc, a velocity dispersion of $\sigma_{\mathrm{clus}} = 0.69 \pm 0.05$ km s^{-1}, and a radial velocity of the centroid of the cluster of $\overline{V}_r = 5.74 \pm 0.07$ km s^{-1}. The total χ_v^2 at the end of the last iteration is 139 for a total of 141 stars, corresponding to 139 degrees of freedom. The distribution of individual contributions to χ_v^2 around the cut-off value of 9 are 6.1, 6.4, 8.0, 10.1, 12.2, 12.6, 25.4, 25.5, 49.9, and 60.6, where we include the first three stars with the values less than 9 as Pleiades members. The individual contributions to χ_v^2 are not distributed as the square of a Gaussian function, and there is a clear break in the distribution around 13, although there is no clear break in the individual $\chi_{v,i}^2$ values at 9. The three stars with individual $\chi_{v,i}^2$ in the range $9 < \chi_{v,i}^2 < 12$ are plausible members,

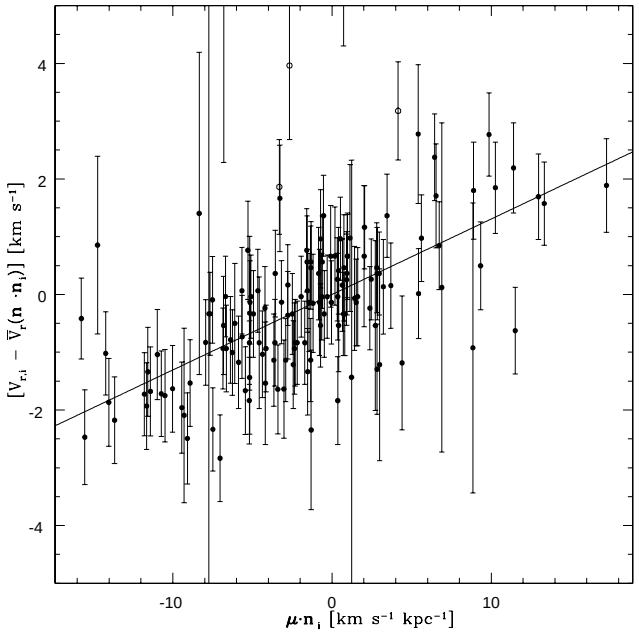

FIG. 2.—Radial velocities of the Pleiades candidates as a function of the scalar product of their mean *Hipparcos* proper-motion vector (μ) and the unit vector toward their position (n_i). The slope of the best-fit straight line is the distance to the Pleiades cluster, $d = 130.7 \pm 11.1$ pc. The filled circles show the cluster members used to fit the straight line, while the open circles represent the stars that are rejected as nonmembers by our algorithm.

while the stars with $\chi^2_{v,i} > 20$ are most likely to be binary systems or nonmembers. We find that if we include these three plausible members, the cluster distance is $d = 132.9 \pm 12.4$ pc, the new velocity dispersion is $\sigma_{\rm clus} = 0.80 \pm 0.07$ km s^{-1}, and the radial velocity of the centroid of the cluster is $\overline{V}_r = 5.80 \pm 0.08$ km s^{-1}. The total χ^2_v is 142 for a total of 144 stars, corresponding to 142 degrees of freedom. This shows that our estimate of the cluster distance is not very sensitive to the uncertainty in the cluster membership, and yields values around $d = 130$ pc as long as we reject the extreme outliers.

Figure 2 shows the radial velocity difference $[V_{r,i} - \overline{V}_r(\boldsymbol{n}\cdot\boldsymbol{n}_i)] \simeq (V_{r,i} - \overline{V}_r)$ for all the Pleiades candidates as a function of the quantity $(\boldsymbol{\mu}\cdot\boldsymbol{n}_i)$. The filled circles show the Pleiades members that are used to fit for the cluster distance, while the open circles represent the stars that are rejected as nonmembers by our algorithm. The solid line shows our best fit to equation (14), and its slope is our estimate for the distance to the Pleiades. We repeat here that the radial velocity gradient method is a geometrical method, which relies on the assumption that the velocity structure of the Pleiades is not significantly affected by rotation.

5. COMPARISON WITH *HIPPARCOS* PARALLAXES

The distance to the Pleiades from the radial velocity gradient method corresponds to a distance modulus of $(m - M) = 5.58 \pm 0.18$ mag. This value agrees very well with the "classical" estimates of the Pleiades distance modulus using main-sequence fitting techniques (Vandenberg & Bridges 1984; Eggen 1986; Vandenberg & Poll 1989; PSSKH98), all of which cluster around 5.60 mag. The discrepancy between the main-sequence fitting distance and the mean *Hipparcos* parallax distance to the Pleiades could arise for one of two reasons.

1. The *Hipparcos* parallaxes of the Pleiades members are systematically in error and are larger on average than their true parallaxes.

2. The isochrones that are used to derive the cluster distance in the main-sequence fitting technique are all systematically too bright, leading to a larger distance for the Pleiades.

The theoretical isochrones are calibrated on the Sun using accurate helioseismological data, and they are mostly used in a differential manner to derive the relative distances to clusters. Furthermore, the distances to other open clusters (e.g., the Hyades and α Per) using the same set of theoretical models are consistent with the *Hipparcos* parallax distances (PSSKH98). Finally, only explanation (1) can account for the marginal discrepancy between the mean *Hipparcos* parallax distance to the Pleiades and the distance derived using the radial velocity gradient method in § 4. The distance modulus to the Pleiades using the rotational modulation stars is also 5.60 ± 0.16 mag (O'Dell, Hendry, & Cameron 1994), marginally larger than the mean *Hipparcos* parallax value and in very good agreement with the values from both the main-sequence fitting and the radial velocity gradient techniques. This consistency between the different independent methods of estimating the distance to the Pleiades, all of which converge on a value of about 5.60 mag, strongly suggests that there may be systematic errors in the *Hipparcos* parallaxes toward the Pleiades. We now extend our analysis to examine the spatial structure of these errors.

Figure 3 shows the difference between $\pi_{\rm Hip}$, the *Hipparcos* parallaxes, and $\pi_{\rm pm}$, the parallaxes predicted using *Hipparcos* proper motions assuming that the members have a common space velocity, as a function of their angular distance from the centroid of the cluster ($|\theta|$), for the 65 Pleiades members that are selected from the *Hipparcos*

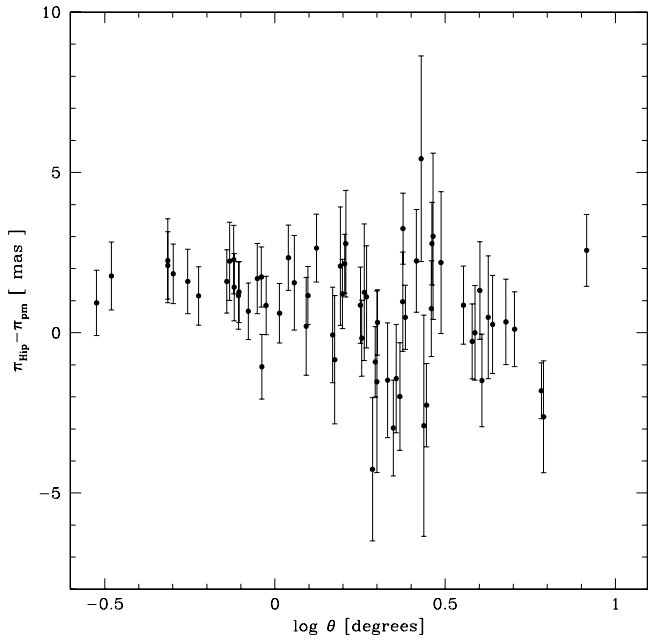

FIG. 3.—Difference between the *Hipparcos* parallaxes of individual stars, $\pi_{\rm Hip}$, and their parallaxes predicted from their *Hipparcos* proper motions assuming a common space velocity for all the cluster members, $\pi_{\rm pm}$, as a function of the angular distance of the stars from the centroid of the cluster ($\theta = |\boldsymbol{\theta}|$). The error bars show the quadrature sum of the errors in $\pi_{\rm Hip}$ and the errors in $\pi_{\rm pm}$.

catalog using the procedure described in § 3.1. The error bars show the quadrature sum of the errors in $\pi_{\rm Hip}$ and the errors in $\pi_{\rm pm}$. It is immediately obvious from this figure that the *Hipparcos* parallaxes are systematically larger than the parallaxes predicted assuming common cluster motion, by up to 2 mas, for all the stars that are located within 1° of the centroid of the cluster. The scatter in the values of $(\pi_{\rm Hip} - \pi_{\rm pm})$ increases for $|\theta| > 1°$, although it is clear that there is still a systematic deviation from zero up to about $|\theta| = 2°$.

Figure 4 shows the contours of the difference between the *Hipparcos* parallaxes $(\pi_{\rm Hip})_s$ smoothed on scales of $\theta_s = 1°$ and the similarly smoothed parallaxes predicted from the *Hipparcos* proper motions assuming a common space velocity for all the cluster members $(\pi_{\rm pm})_s$, in an 8° × 8° region about the centroid of the Pleiades cluster. Solid contours correspond to $(\pi_{\rm Hip} - \pi_{\rm pm})_s \geq 0$, while dashed contours correspond to $(\pi_{\rm Hip} - \pi_{\rm pm})_s < 0$. The light contours range from −1.8 mas to +2 mas in steps of 0.1 mas, while the heavy contours range from −1 mas to +2 mas in steps of 1 mas. The filled circles show the positions of the individual Pleiades members. We find this smoothed parallax difference field by computing the quantity $(\pi_{\rm Hip} - \pi_{\rm pm})$ for each of the 65 Pleiades members and convolving this difference with a Gaussian filter $\exp(-\theta^2/2\theta_s^2)/\sigma_{\rm tot}^2$, where $\sigma_{\rm tot}^2 = \sigma_{\rm Hip}^2 + \sigma_{\rm pm}^2$. The weighting by the inverse of the square of the error ensures that the stars with noisy estimates of the parallax difference are naturally given low weights when computing the smoothed parallax difference field. This figure clearly shows that the *Hipparcos* parallaxes $\pi_{\rm Hip}$ are systematically larger than $\pi_{\rm pm}$ by up to 2 mas, throughout the inner 6° × 6° region around the centroid of the Pleiades. Since very few of our 65 cluster members are located outside the inner 4° × 6° region, the smoothed field values (the signal) outside this region comes primarily from the stars in the inner region and therefore contains very little independent information about the spatial structure of the systematic errors. Hence, we restrict our quantitative analysis of this parallax difference field of the Pleiades to the inner 4° × 6° region (shown by the dashed box in Fig. 4) in the remainder of this paper.

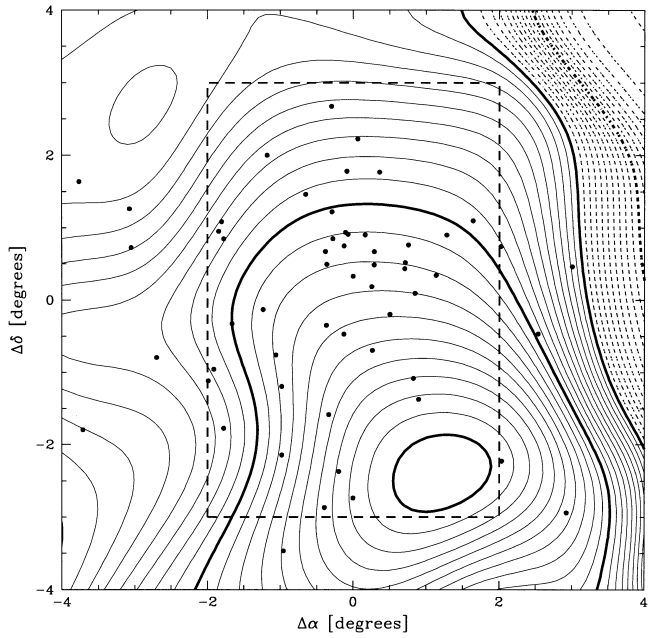

FIG. 4.—Contours of the difference between the *Hipparcos* parallaxes $(\pi_{\rm Hip})_s$ smoothed on a scale of $\theta_s = 1°$ and the similarly smoothed parallaxes predicted from the *Hipparcos* proper motions assuming a common space velocity for all the Pleiades members $(\pi_{\rm pm})_s$, in an 8° × 8° region about the centroid of the Pleiades cluster. Solid contours correspond to $(\pi_{\rm Hip} - \pi_{\rm pm})_s \geq 0$, while dashed contours correspond to $(\pi_{\rm Hip} - \pi_{\rm pm})_s < 0$. The light contours range from −1.8 mas to +2 mas in steps of 0.1 mas, while the heavy contours range from −1 mas to +2 mas in steps of 1 mas. The filled circles show the positions of the individual Pleiades members. The dashed box shows the inner 4° × 6° region about the centroid of the Pleiades cluster.

The spatial structure seen in Figure 4 can arise from spatially correlated systematic errors in (1) the *Hipparcos* parallaxes $\pi_{\rm Hip}$, (2) the parallaxes predicted from the *Hipparcos* proper motions assuming a common space velocity for all the cluster members $\pi_{\rm pm}$, or (3) both of these parallaxes. Of these three possibilities, (1) will be true if there are as yet uncorrected spatial correlations in the *Hipparcos* parallax errors on angular scales of a few degrees, while (2) will be the main source of error if the velocity field of the Pleiades is dominated by substantial substructures that invalidate the assumption of a common space velocity for all the cluster members. In principle, it is also possible that the structure arises from spatially correlated errors in the *Hipparcos* proper motions. Indeed, if there are spatially correlated errors in *Hipparcos* parallaxes, it is reasonable to expect similar effects in the *Hipparcos* proper motions. However, the structures seen in Figure 4 are of the same size (∼1 mas) as σ_π(Hip), the statistical errors in $\pi_{\rm Hip}$. The statistical errors in $\pi_{\rm pm}$ arising from σ_μ(Hip), the errors in the *Hipparcos* proper motions, are smaller than this by a factor $(\sigma_\mu/\mu)/(\sigma_\pi/\pi) \approx \frac{1}{6}$. Hence, one does not a priori expect correlations among the *Hipparcos* proper-motion errors to have a noticeable effect. Nevertheless, the tests that we carry out below would automatically detect this unexpected effect if it were present.

To check which of the three alternatives is correct, we plot the quantities $(\pi_{\rm Hip} - \langle\pi_{\rm Hip}\rangle)_s$ and $(\pi_{\rm pm} - \langle\pi_{\rm pm}\rangle)_s$ in Figures 5 and 6, respectively, in the same format as in Figure 4. Here, $\langle\pi_{\rm Hip}\rangle = 8.52 \pm 0.15$ mas and $\langle\pi_{\rm pm}\rangle = 7.63 \pm 0.03$ mas are the average values, computed using the 65 Pleiades members, of the *Hipparcos* parallaxes and the parallaxes predicted assuming a common space velocity for all the cluster members. The structures in Figure 5 closely resemble those in Figure 4 except for a shift of the zero point caused by the adoption of $\langle\pi_{\rm Hip}\rangle$ as the Pleiades cluster parallax. In Figure 6, on the other hand, the inner 4° × 4° region around the cluster center is remarkably smooth and close to zero, and there are no contours (either positive or negative) other than the one corresponding to $(\pi_{\rm pm} - \langle\pi_{\rm pm}\rangle)_s = 0$. This shows that the structures in $\pi_{\rm pm}$ arising from the errors in the *Hipparcos* proper motions are quite small compared to the structures arising from the correlations in the *Hipparcos* parallaxes.

It is clear from Figures 5 and 6 that the spatial structure in Figure 4 arises primarily from the spatial structure in the *Hipparcos* parallaxes. The parallaxes in the entire region southeast of the centroid of the cluster are systematically too large by up to 2 mas, while there are no regions inside the inner 4° × 6° region where the parallax difference is less than −0.5 mas. It is clear from Figure 4 that an average of the *Hipparcos* parallaxes of stars lying in this region will be systematically larger, leading to an underestimate of the distance to the Pleiades. We note here that the spatial structure seen in the $(\pi_{\rm Hip} - \pi_{\rm pm})_s$ field in Figure 4 is independent

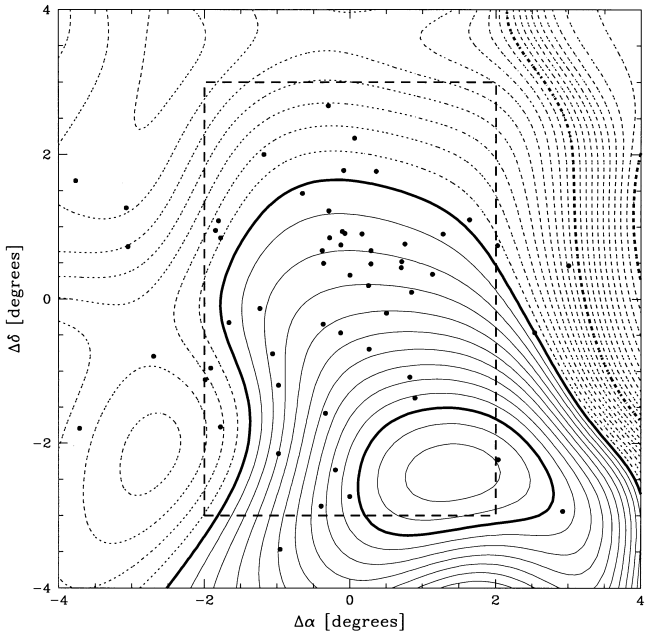

FIG. 5.—Contours of the difference between the smoothed *Hipparcos* parallaxes $(\pi_{\rm Hip})_s$ and the mean *Hipparcos* parallax of the 65 Pleiades cluster members, $\langle\pi_{\rm Hip}\rangle$. Solid contours correspond to $(\pi_{\rm Hip} - \langle\pi_{\rm Hip}\rangle)_s \geq 0$, while dashed contours correspond to $(\pi_{\rm Hip} - \langle\pi_{\rm Hip}\rangle)_s < 0$. The light contours range from -2 mas to $+2.2$ mas in steps of 0.1 mas, while the heavy contours range from -2 mas to $+2$ mas in steps of 1 mas. The filled circles show the positions of the individual Pleiades members. The dashed box shows the inner $4^\circ \times 6^\circ$ region about the centroid of the Pleiades cluster.

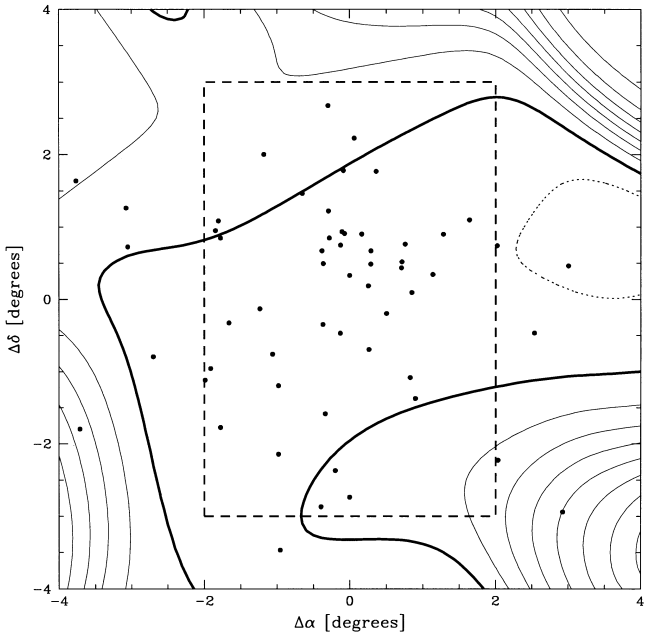

FIG. 6.—Contours of the difference between the smoothed parallaxes predicted using the *Hipparcos* proper motions assuming a common cluster space velocity for the members $(\pi_{\rm pm})_s$ and the mean value of this quantity for the 65 Pleiades members, $\langle\pi_{\rm pm}\rangle$. Solid contours correspond to $(\pi_{\rm pm} - \langle\pi_{\rm pm}\rangle)_s \geq 0$, while dashed contours correspond to $(\pi_{\rm pm} - \langle\pi_{\rm pm}\rangle)_s < 0$. The light contours range from -0.1 mas to $+0.7$ mas in steps of 0.1 mas, while the heavy line represents the contour corresponding to $(\pi_{\rm pm} - \langle\pi_{\rm pm}\rangle)_s = 0$. The filled circles show the positions of the individual Pleiades members. The dashed box shows the inner $4^\circ \times 6^\circ$ region about the centroid of the Pleiades cluster.

of our distance scale to the Pleiades itself. Thus, if our estimate of the Pleiades space velocity is wrong, so that all of our estimates of $\pi_{\rm pm}$ are systematically in error, the absolute levels of the contours will change, while the spatial structure itself will remain the same. A one-dimensional analog of our Figure 5 is Figure 20 of PSSKH98, which plots the *Hipparcos* parallaxes of individual Pleiades members as a function of their angular distance from the cluster center.

We see from the spatial structure in the smoothed field $(\pi_{\rm Hip} - \pi_{\rm pm})_s$ in Figure 4 that the *Hipparcos* parallax errors are correlated with position on angular scales of about 3°, with an amplitude of up to 2 mas. This is much larger than the upper limit of 0.1 mas to the error in the global zero point of the *Hipparcos* parallaxes (Arenou et al. 1995, 1997), which, however, is valid only on large angular scales. Our estimate of the systematic errors demonstrates that they could be an order of magnitude larger than this on small angular scales, as was already suggested by PKSSH98.

Even before the launch of the *Hipparcos* satellite, it was anticipated that the errors in the *Hipparcos* parallaxes would be correlated over angular scales of a few degrees (Hoyer et al. 1981; Lindegren 1988, 1989). The analysis of the *Hipparcos* parallaxes showed that the parallax errors are indeed strongly correlated on small scales, although the correlation becomes negligible for angular separations greater than about 4° (Lindegren et al. 1997; Arenou 1997; van Leeuwen & Evans 1998). An empirical fit to this correlation is given by the function (Lindegren et al. 1997)

$$R(\theta) = R(0)\,\exp\,(-0.14\theta - 1.04\theta^2 + 0.41\theta^3 - 0.06\theta^4)\,, \tag{16}$$

where the angular separation, θ, is measured in degrees, and $R(0) = 0.59$. We now estimate how likely it is to get a parallax difference map $(\pi_{\rm Hip} - \pi_{\rm pm})_s$ with the severe fluctuations seen in Figure 4 if the errors in $\pi_{\rm Hip}$ are correlated according to equation (16).

Figure 7 shows the normalized distribution of the fluctuation amplitude, A, in the quantity $(\pi_{\rm Hip} - \pi_{\rm pm})_s$, if the errors in *Hipparcos* parallaxes are correlated over small angular scales as described by equation (16). We define A as

$$A = [\langle(\pi_{\rm Hip} - \pi_{\rm pm})_s^2\rangle - \langle(\pi_{\rm Hip} - \pi_{\rm pm})_s\rangle^2]^{1/2}\,. \tag{17}$$

We compute this distribution of A from an ensemble of 5000 Monte Carlo realizations of the parallax differences $(\pi_{\rm Hip} - \pi_{\rm pm})_s$. At each Monte Carlo experiment, we assign a value of $(\pi_{{\rm Hip},i} - \pi_{{\rm pm},i})$ to each of the 65 members that is drawn from a Gaussian distribution whose variance is $\sigma^2_{{\rm tot},i} = \sigma^2_{\pi,i}({\rm Hip}) + \sigma^2_{\pi,i}({\rm pm})$ and whose correlation with the other stars is described by equation (16). We then compute A using only the values of the smoothed parallax difference field within the inner $4^\circ \times 6^\circ$ region of the centroid of the cluster. The arrow in Figure 7 shows the value of the observed fluctuation amplitude in the same region, $A_{\rm obs} = 0.47$ mas, for the field shown in Figure 4. The probability of obtaining a fluctuation amplitude greater than the observed value is $P(A > A_{\rm obs}) = 17.7\%$, if the errors in the *Hipparcos* parallaxes are correlated according to equation (16).

There is a small but finite probability that the fluctuation amplitude of the smoothed parallax differences $(\pi_{\rm Hip} - \pi_{\rm pm})_s$ toward the Pleiades is as high as that seen in Figure 4. However, the modest probability of 17.7% suggests that there might be angular correlations in the *Hipparcos* parallax errors over and the above the correlation

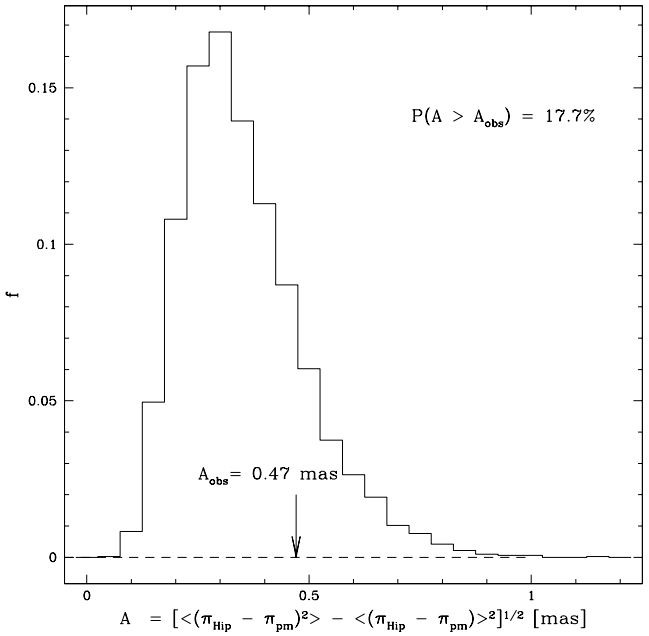

FIG. 7.—Normalized distribution of the fluctuation amplitude, A, in the difference between the smoothed *Hipparcos* parallaxes $(\pi_{\rm Hip})_s$ and the parallaxes predicted from the *Hipparcos* proper motions assuming a common space velocity for all the Pleiades members $(\pi_{\rm pm})_s$, in a $4^\circ \times 6^\circ$ region about the center of the Pleiades cluster. This distribution is computed assuming that the parallax differences for each of the $i = 1, 2, \ldots 65$ Pleiades members are distributed as a Gaussian function whose variance is $\sigma^2_{{\rm tot},i} = \sigma^2_{\pi,i}({\rm Hip}) + \sigma^2_{\pi,i}({\rm pm})$ and whose correlation with the other stars is described by eq. (16). The arrow shows the observed fluctuation amplitude in the same region, $A_{\rm obs} = 0.47$ mas, for the field shown in Fig. 4.

described by equation (16). We now check to see if there is additional evidence for these extra correlations in the *Hipparcos* parallax errors toward the Hyades open cluster.

6. SYSTEMATIC ERRORS TOWARD HYADES

The analysis in the previous section shows that the *Hipparcos* parallax errors toward the Pleiades cluster are spatially correlated over angular scales of a few degrees, beyond what is expected from the analysis of the entire *Hipparcos* catalog. We now check to see if these extra angular correlations are also present in the *Hipparcos* parallax errors toward the Hyades. If we do find extra correlations toward the Hyades, it is possible that these correlations are generic features of the *Hipparcos* parallax errors all over the sky. We describe our selection of Hyades members from the *Hipparcos* catalog in § 6.1 and analyze the systematics of their *Hipparcos* parallax errors in § 6.2

6.1. *Hyades Membership*

We start by selecting a sample of stars from the *Hipparcos* catalog that are likely to be Hyades members based on their *Hipparcos* proper motions, using the procedure described in § 3.1. We assume that the centroid of the Hyades cluster is at a distance of 46.5 pc toward the direction $\alpha = 04^{\rm h}26^{\rm m}32^{\rm s}$, $\delta = 17^\circ 13'.3$ (2000), the velocity dispersion of the cluster is $\sigma_{\rm clus} = 320$ m s^{-1}, and the bulk velocity of the cluster in equatorial coordinates is $(V_x, V_y, V_z) = (-5.41, 45.45, 5.74)$ km s^{-1}, as determined by NG99 using the statistical parallax algorithm. For each star that is within 30° of this direction, we form the quantity χ^2_i as defined in equation (10) and select the stars whose χ^2_i is less than 9 to be Hyades candidates. We adopt a value of the distance dispersion $\theta_d \equiv (\delta d/d) = 15\%$ to account for the finite depth of the cluster. This procedure selects a total of 204 Hyades candidates from the *Hipparcos* catalog. We use equation (12) to predict the parallaxes (and the associated errors) of these Hyades candidates from their *Hipparcos* proper motions, assuming that all the cluster members move with the same space velocity. We estimate the absolute magnitudes of these stars using the parallaxes derived in this manner and their apparent V_J magnitudes from Tycho photometry.

Figure 8 shows the color-magnitude diagram of these Hyades candidates. We have plotted only the 197 candidates whose absolute magnitude errors are less than 1 mag. We see that there is an obvious main sequence, and there are a few stars lying above and below it. These are most likely to be nonmembers. We see that the main sequence in the color range $0.1 < (B-V)_J < 0.6$ has a steeper slope and a larger width compared to that in the color range $0.6 < (B-V)_J < 1.5$. The larger width on the blue side probably arises from unidentified binary systems. Accordingly, we fit different color-magnitude relations in each of these color ranges and select all the Hyades candidates that lie within a finite width of these relations as Hyades members. Our color-magnitude relation for the Hyades is

$$M_V = \begin{cases} 2.72 + 7.14[(B-V)_J - 0.35]\,, & \text{if } 0.1 < (B-V)_J < 0.6\,, \\ 6.44 + 4.84[(B-V)_J - 1.00]\,, & \text{if } 0.6 < (B-V)_J < 1.5\,. \end{cases} \quad (18)$$

The solid line in the figure shows this relation. We assume that all the stars that lie within 0.4 mag of the blue CMD

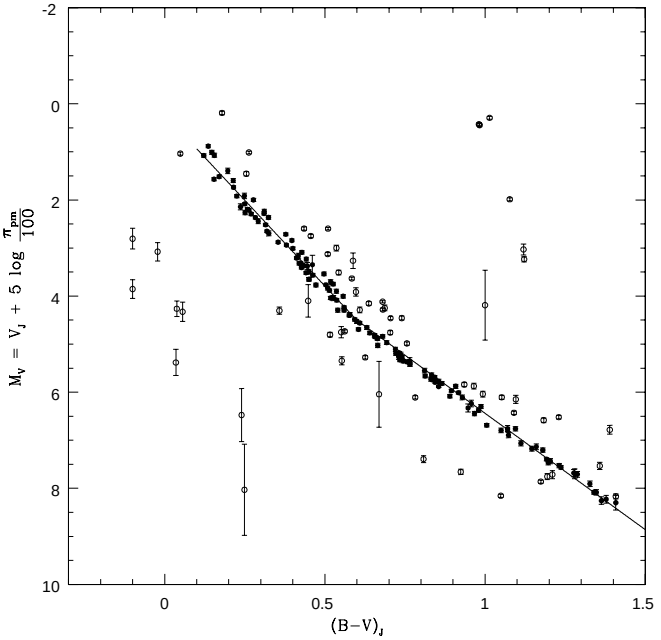

FIG. 8.—Color-magnitude diagram (CMD) of the 197 stars in the *Hipparcos* catalog whose individual proper motions are consistent with them being Hyades members and whose absolute magnitude errors are smaller than 1 mag. The parallax to each star is estimated from its *Hipparcos* proper motion, assuming a common space velocity for all the Hyades cluster members. The filled circles show the stars that are most likely to be Hyades members based on their location in the CMD, while the open circles represent nonmembers and plausible binaries. The solid line shows our fit for the color-magnitude relation of the Hyades. The colors and the apparent magnitudes $(B-V)_J$ and V_J are taken from Tycho photometry.

relation, or within 0.24 mag of the red CMD relation, are Hyades members. The 132 Hyades members selected by this procedure are represented by the filled circles, while the nonmembers and plausible binaries are shown by the open circles.

6.2. *Systematics in Hipparcos Parallaxes*

Figure 9 shows the contours of the difference between the *Hipparcos* parallaxes $(\pi_{\rm Hip})_s$ smoothed on scales of $\theta_s = 1^\circ$ and the similarly smoothed parallaxes predicted from the *Hipparcos* proper motions assuming a common space velocity for all the cluster members $(\pi_{\rm pm})_s$, in an $8^\circ \times 8^\circ$ region about the centroid of the Hyades cluster. This figure for the Hyades is analogous to Figure 4 for the Pleiades. We find this smoothed parallax difference field using the 132 Hyades members, in the same manner as described in § 5 for the Pleiades.

The smoothed parallax difference field in Figure 9 clearly shows that the *Hipparcos* parallaxes $\pi_{\rm Hip}$ toward the Hyades are also spatially correlated over angular scales of a few degrees, with an amplitude of about 1–2 mas. We have also plotted (but do not show) the quantities $(\pi_{\rm Hip} - \langle\pi_{\rm Hip}\rangle)_s$ and $(\pi_{\rm pm} - \langle\pi_{\rm pm}\rangle)_s$ for the Hyades, in a manner similar to Figures 5 and 6 for the Pleiades. Once again, we find that the spatial structure in Figure 9 arises from the structure in the *Hipparcos* parallaxes toward the Hyades and is not due to the structure in $(\pi_{\rm pm})_s$. However, unlike the *Hipparcos* parallaxes toward the Pleiades, which were all too large in the entire inner $4^\circ \times 6^\circ$ region, the *Hipparcos* parallaxes toward the Hyades are systematically larger in some regions [e.g., a region of $2^\circ \times 2^\circ$ centered on $(\Delta\alpha, \Delta\delta) = (+3^\circ, -1^\circ)$] and systematically smaller in other regions [e.g., a region of $2^\circ \times 2^\circ$ centered on $(\Delta\alpha, \Delta\delta) = (-1^\circ, 1\overset{\circ}{.}5^\circ)$]. Hence, the average value of the parallax difference is close to zero, when it is computed using all the Hyades members that lie in different regions. This, combined with the large angular size of the Hyades cluster, can explain why the main-sequence fitting distance to the Hyades agrees with the average of the *Hipparcos* parallaxes of its members (PSSKH98), although there are significant spatial correlations in the *Hipparcos* parallax errors of the individual Hyades members.

Figure 10 shows the normalized distribution of the fluctuation amplitude, A, in the quantity $(\pi_{\rm Hip} - \pi_{\rm pm})_s$, if the errors in *Hipparcos* parallaxes are correlated according to equation (16). We compute this distribution in the same manner as described for the Pleiades cluster. We compute the fluctuation amplitude only within the inner $6^\circ \times 8^\circ$ region (*dashed box*, Fig. 9) around the centroid of the Hyades. The arrow in Figure 10 shows the value of the observed fluctuation amplitude in the same region, $A_{\rm obs} = 0.62$ mas, for the field shown in Figure 9. The probability of obtaining a fluctuation amplitude greater than the observed value is $P(A > A_{\rm obs}) = 9.1\%$.

We see that there is only a modest probability of obtaining a fluctuation amplitude that is as large as the observed value. This is similar to the case of the Pleiades, although the probability in the case of the Hyades is almost a factor of two smaller than that for the Pleiades. The joint prob-

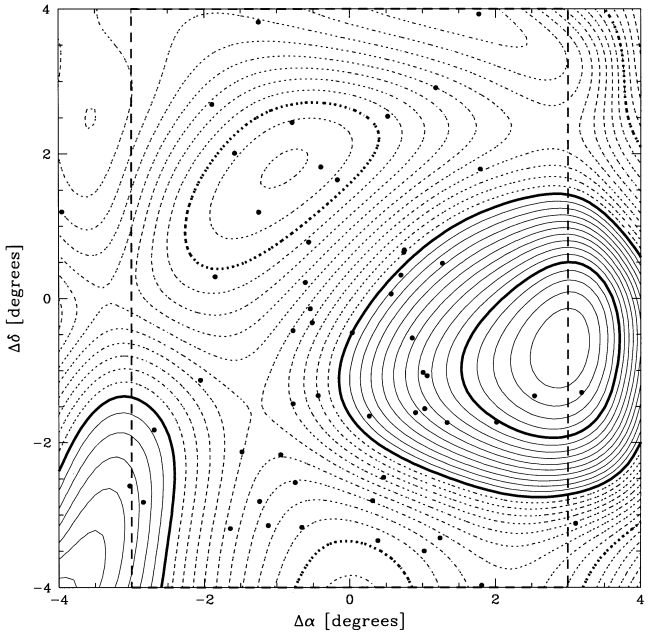

FIG. 9.—Contours of the difference between the *Hipparcos* parallaxes $(\pi_{\rm Hip})_s$ smoothed on a scale of $\theta_s = 1^\circ$ and the similarly smoothed parallaxes predicted from the *Hipparcos* proper motions assuming a common space velocity for all the Hyades members $(\pi_{\rm pm})_s$, in an $8^\circ \times 8^\circ$ region about the centroid of the Hyades cluster. Solid contours correspond to $(\pi_{\rm Hip} - \pi_{\rm pm})_s \geq 0$, while dashed contours correspond to $(\pi_{\rm Hip} - \pi_{\rm pm})_s < 0$. The light contours range from -1.4 mas to $+1.4$ mas in steps of 0.1 mas, while the heavy contours range from -1 mas to $+1$ mas in steps of 1 mas. The filled circles show the positions of the individual Hyades members. The dashed box shows the inner $6^\circ \times 8^\circ$ region about the centroid of the Hyades cluster.

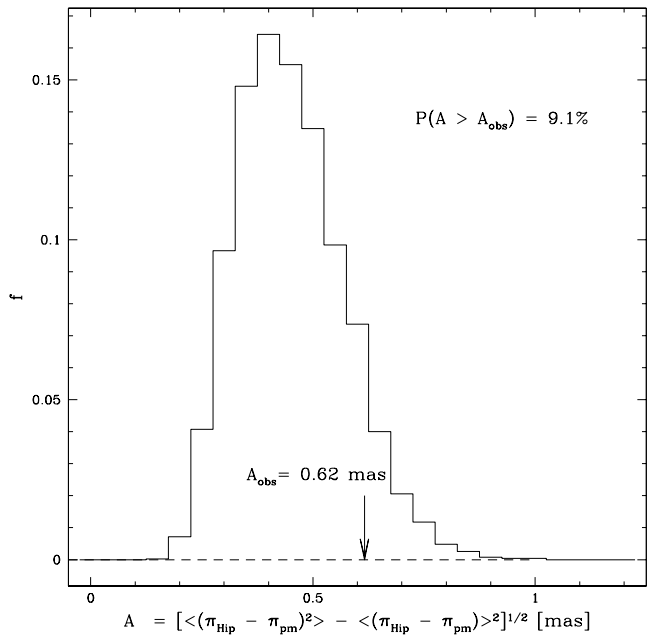

FIG. 10.—Normalized distribution of the fluctuation amplitude, A, in the difference between the smoothed *Hipparcos* parallaxes $(\pi_{\rm Hip})_s$ and the parallaxes predicted from *Hipparcos* proper motions assuming a common space velocity for all the Hyades members $(\pi_{\rm pm})_s$, in a $6^\circ \times 8^\circ$ region about the center of the Hyades cluster. This distribution is computed assuming that the parallax differences for each of the $i = 1, 2, \ldots 132$ Hyades members are distributed as a Gaussian function whose variance is $\sigma^2_{{\rm tot},i} = \sigma^2_{\pi,i}({\rm Hip}) + \sigma^2_{\pi,i}({\rm pm})$ and whose correlation with the other stars is described by eq. (16). The arrow shows the observed fluctuation amplitude in the same region, $A_{\rm obs} = 0.62$ mas, for the field shown in Fig. 9.

ability of obtaining the observed fluctuation amplitudes for both the Pleiades and the Hyades is only about 1.6%, if the smoothed parallax differences of the Pleiades and the Hyades clusters are independent random processes. This supports our speculation that there might be stronger angular correlations in the *Hipparcos* parallax errors, beyond the model described by equation (16).

7. CONCLUSIONS

The *Hipparcos* mission has derived absolute trigonometric parallaxes to about 120,000 stars distributed all over the sky. It is the largest homogeneous all-sky source of absolute parallaxes to date and can potentially influence many branches of astronomy (see the review by Kovalevsky 1998). Therefore, it is crucial to understand the errors in the *Hipparcos* astrometry. Motivated by the increasing evidence that the distances to some open clusters inferred from the mean *Hipparcos* parallaxes of their members are in conflict with their pre-*Hipparcos* values, we have critically analyzed the spatial correlations of the *Hipparcos* parallax errors on small scales. Specifically, we have compared the *Hipparcos* parallaxes of the Pleiades and the Hyades cluster members with their parallaxes predicted from their *Hipparcos* proper motions, assuming that all the cluster members move with the same space velocity.

Our main conclusions are as follows.

1. We have derived a distance modulus to the Pleiades of $(m - M) = 5.58 \pm 0.18$ mag using a variant of the moving cluster method—the gradient in the radial velocity of the cluster members in the direction of the proper motion of the cluster. This value agrees very well with the distance modulus of 5.60 ± 0.04 mag derived using the classical main-sequence fitting technique (Vandenberg & Poll 1989; PSSKH98), but it is in marginal conflict with the shorter distance modulus of 5.33 ± 0.06 mag inferred by averaging the *Hipparcos* parallaxes of Pleiades members (van Leeuwen & Ruiz 1997). The radial velocity gradient method to estimate the cluster distance is a geometrical technique that relies on the assumption that the velocity structure of the Pleiades is not significantly affected by rotation.

2. We find that the *Hipparcos* parallax errors toward the Pleiades cluster are spatially correlated over angular scales of 2°–3°, with an amplitude of up to 2 mas. This can explain why the distance to the Pleiades cluster inferred by averaging the *Hipparcos* parallaxes of its members is smaller than its distance inferred by other techniques. Even if the velocity distribution of the Pleiades members do not conform to a common bulk space motion, we still see the spatial correlations in the *Hipparcos* parallaxes. However, we cannot determine the zero point of these fluctuations without the independent estimate of the cluster distance that comes from the assumption of a common space velocity for all the cluster members (or some other parallax-independent source).

3. The spatial correlations in the *Hipparcos* parallaxes are also seen toward the Hyades cluster. However, there are both positive and negative fluctuations in the *Hipparcos* parallax errors toward the region of the Hyades, with the result that these fluctuations cancel out on average and the distance to the Hyades inferred by averaging the *Hipparcos* parallaxes of all its members agrees well with other distance measurements.

4. The probabilities of obtaining the observed fluctuation amplitudes, $A_{\rm obs}$, in the smoothed parallax difference field $(\pi_{\rm Hip} - \pi_{\rm Hip})_s$, are small for both the Pleiades and the Hyades (17.7% and 9.1%, respectively), if the angular correlations in the *Hipparcos* parallax errors are described by equation (16). This suggests that there are almost certainly stronger spatial correlations in the *Hipparcos* parallax errors beyond what is modeled by equation (16). Since we see these stronger correlations in *Hipparcos* parallax errors toward both the Pleiades and the Hyades, we suggest that this may be a generic feature of the *Hipparcos* parallax errors all over the sky.

It is clear from the above conclusions that it is necessary to adopt a cautious approach when averaging the *Hipparcos* parallaxes over small angular scales. In particular, it is necessary to quantify the effect of spatial correlations in the parallaxes when dealing with a distribution of stars that are separated by a few degrees. Thus, for example, it has been found that when *Hipparcos* parallaxes are used to estimate the absolute magnitudes of stars in open clusters, such disparate open clusters as Praesepe, Coma Ber, α Per and Blanco I define the same main sequence despite their widely different metallicities, with [Fe/H] ranging from -0.07 dex for Coma Ber to about $+0.23$ dex for Blanco I (Mermilliod et al. 1997b; Robichon et al. 1997). Our analysis shows that such an effect could arise from spatially correlated *Hipparcos* parallaxes of the cluster members, of the type seen toward the Pleiades and the Hyades clusters. Thus, a metal-rich cluster whose *Hipparcos* parallaxes are all systematically larger than the true values can have the same apparent main sequence as a metal-poor cluster whose systematic errors in different regions of the cluster cancel out on an average. The discrepancy between the distances inferred from the average *Hipparcos* parallax and that inferred from the main-sequence fitting technique for other open clusters (e.g., for Coma Ber, PSSKH98) could also arise from correlated parallax errors that do not cancel out on average, similar to the situation in the Pleiades. On the other hand, as we showed for the Hyades, an agreement between these two distance measurements does not necessarily preclude stronger spatial correlations in the *Hipparcos* parallaxes.

Our work shows that there are strong spatial correlations in the errors of the parallaxes in the *Hipparcos* catalog. We note that this is not necessarily in conflict with the upper limit of 0.1 mas to the error in the global zero point of the *Hipparcos* parallaxes over the full sky (Arenou et al. 1995, 1997). The global tests have very little power to probe for systematic errors on smaller scales. Finally, we note that, given the sparse average density of about 3 stars arcsec^{-2} in the *Hipparcos* catalog, the open clusters with a large local concentration of stars may be the only regions where we can test the small scale systematics in the *Hipparcos* catalog.

After the completion of this work, we became aware of the work of van Leeuwen (1999), who has suggested the existence of an age-luminosity relation for main-sequence stars, in strong contradiction with the standard theory of stellar evolution. Alternatively, if the small-angle correlations in the *Hipparcos* parallaxes toward the Pleiades and the Hyades that we found in this paper are a generic feature of *Hipparcos* parallaxes, then this proposed age-luminosity relation could be an artifact arising from an inadequate

treatment of these correlations. A more detailed discussion of this issue is beyond the scope of this paper and will be addressed in the ongoing work of Pinsonneault et al. (1999).

This work was supported in part by the grant AST 97-27520 from the NSF. We thank Marc Pinsonneault, Bob Hanson, John Stauffer, and Frederic Arenou for helpful suggestions. We also thank David Weinberg for his comments on an earlier draft of this paper.

REFERENCES

Alexander, J. B. 1986, MNRAS, 220, 473
Arenou, F. 1997, in *Hipparcos* and Tycho Catalogues, Vol. 3, Construction of the *Hipparcos* Catalogue, ESA SP-1200 (Noordwijk: ESA), 369
Arenou, F., Lindegren, L., Froeschle, M., Gomez, A. E., Turon, C., Perryman, M. A. C., & Wielen, R. 1995, A&A, 304, 52
Arenou, F., Mignard, F., & Palasi, J. 1997, in *Hipparcos* and Tycho Catalogues, Vol. 3, Construction of the *Hipparcos* Catalogue, ESA SP-1200 (Noordwijk: ESA), 433
Artyukhina, N. M., & Kalinina, E. 1970, Tr. Shternberg Astron. Inst., 39, 111
Boss, L. 1908, AJ, 26, 31
Bouvier, J., Rigaut, F., & Nadeau, D. 1997, A&A, 320, 74
Crawford, D. L. 1975, AJ, 80, 955
Detweiler, H. L., Yoss, K. M., Radick, R. R., & Becker, S. A. 1984, AJ, 89, 1038
Dravins, D., Larsson, B., & Nordlund, A. 1986, A&A, 158, 83
ESA. 1997, *Hipparcos* and Tycho Catalogues, Vol. 3, The *Hipparcos* and Tycho Catalogues, ESA SP-1200 (Noordwijk: ESA)
Eggen, O. J. 1986, PASP, 96, 755
Gunn, J. E., Griffin, R. F., Griffin, R. E. M., & Zimmerman, B. A. 1988, AJ, 96, 198
Hertzsprung, E. 1947, Ann. Sterrew. Leiden, 19, 3
Hoyer, P., Poder, K., Lindegren , L., & Hog, E. 1981, A&A, 101, 228
Kovalevsky, J. 1998, ARA&A, 36, 99
Lindegren, L. 1988, in Scientific Aspects of the Input Catalog Preparation II, ed. J. Torra & C. Turon (Noordwijk: ESA), 179
———. 1989, in *Hipparcos* Mission, ESA SP-1111, Vol. III, ed. M. A. C. Perryman et al. (Noordwijk: ESA), 311
———. 1995, A&A, 304, 61
Lindegren, L., Froeschle, M., & Mignard, F. 1997, *Hipparcos* and Tycho Catalogues, Vol. 3, Construction of the *Hipparcos* Catalogue, ESA SP-1200 (Noordwijk: ESA), 323
Mermilliod, J. C., Bratschi, P., & Mayor, M. 1997a, A&A, 320, 74
Mermilliod, J. C., Rosvick, J. M., Duquennoy, A., & Mayor, M. 1992, A&A, 265, 513
Mermilliod, J.-C., Turon, C., Robichon, N., Arenou, F., & Lebreton, Y. 1997b, in *Hipparcos* Venice 1997, ed. B. Battrick & M. A. C. Perryman (Noordwijk: ESA), 643
Nadeau, D. 1988, ApJ, 325, 480
Narayanan, V. K., & Gould, A. 1999, ApJ, 515, 256 (NG99)
Nissen, P. E. 1988, A&A, 199, 146
O'Dell, M. A., Hendry, M. A., & Cameron, A. C. 1994, MNRAS, 268, 181
Perryman, M. A. C., et al. 1998, A&A, 331, 81
Pinsonneault, M. H., Stauffer, J., Soderblom, D. R., King, J. R., & Hanson, R. B. 1998, ApJ, 504, 170 (PSSKH98)
Pinsonneault, M. H., et al. 1999, in preparation
Raboud, D., & Mermilliod, J. C. 1998, A&A, 329, 101
Robichon, N., Arenou, F., Turon, C., Mermilliod, J.-C.,& Lebreton, Y. 1997, in *Hipparcos* Venice 1997, ed. B. Battrick & M. A. C. Perryman (Noordwijk: ESA), 567
Rosvick, J. M., Mermilliod, J. C., & Mayor, M. 1992a, A&A, 255, 130
———. 1992b, A&A, 259, 720
Schwan, H. 1991, A&A, 243, 386
Soderblom, D. R., King, J. R., Hanson, R. B., Jones, B. F., Fischer, D., Stauffer, J. R., & Pinsonneault, M. H. 1998, ApJ, 504, 192
Stromgren, B., Olsen, E. H., & Gustafsson, B. 1982, PASP, 94, 5
Thackeray, A. D. 1967, in IAU Symp. 30, Determination of Radial Velocities and Their Applications, ed. A. H. Batten & Heard, J. H (New York: Academic), 163
Vandenberg, D. A., & Bridges, T. J. 1984, ApJ, 278, 679
Vandenberg, D. A., & Poll, H. E. 1989, AJ, 98, 4
van Leeuwen, F. 1999, A&A, 341, L71
van Leeuwen, F., Alphenaar, P., & Brand, J. 1986, A&AS, 65, 309
van Leeuwen, F., & Evans, D. W. 1998, A&AS, 130, 157
van Leeuwen, F., & Ruiz, C. S. H. 1997, in *Hipparcos* Venice 1997, ed. B. Battrick & M. A. C. Perryman (Noordwijk: ESA), 689